Patient-Specific Modeling and Analysis of the Mitral Valve Using 3D-TEE

Philippe Burlina[1,2], Chad Sprouse[1], Daniel DeMenthon[1], Anne Jorstad[1], Radford Juang[1], Francisco Contijoch[3], Theodore Abraham[4], David Yuh[5], and Elliot McVeigh[3]

[1] Johns Hopkins University Applied Physics Laboratory
[2] Dept. of Computer Science
[3] Dept. of Biomedical Engineering, School of Medicine
[4] Division of Cardiology
[5] Division of Cardiac Surgery, Baltimore, MD, USA

Abstract. We describe a system dedicated to the analysis of the complex three-dimensional anatomy and dynamics of an abnormal heart mitral valve using three-dimensional echocardiography to characterize the valve pathophysiology. This system is intended to aid cardiothoracic surgeons in conducting preoperative surgical planning and in understanding the outcome of "virtual" mitral valve repairs. This paper specifically addresses the analysis of three-dimensional transesophageal echocardiographic imagery to recover the valve structure and predict the competency of a surgically modified valve by computing its closed state from an assumed open configuration. We report on a 3D TEE structure recovery method and a mechanical modeling approach used for the valve modeling and simulation.

Keywords: Mitral valvuloplasty, patient specific modeling, 3D echocardiography, preoperative surgical planning.

1 Introduction

This paper addresses the problem of exploiting 3D Transesophageal Echocardiographic data (3D TEE) to recover the structure of the mitral valve and surrounding left heart anatomy, and to model the valve pathophysiology. The tools we are designing can be applied in cardiothoracic surgery (to develop systems aiding in preoperative valvuloplasty planning), in cardiology (for performing diagnostics), and for education and training of ultrasonographers and anesthesiologists (often responsible for intraoperative TEE acquisition). The mitral valve is an essential structure which ensures unidirectional blood flow from the left atrium to the left ventricle. One of the essential issues in characterizing valve pathologies and planning surgical valve reconstruction is the ability to predict the outcome of a given valvuloplasty surgical procedure. There are many options for valvuloplasty including the addition of a ring, the resection of part of the valve leaflets, or modifications to the chordae tendinae.

Valvuloplasty surgery involves cardiopulmonary bypass. A bypass procedure has associated risks which require that the surgeon make a decision within a relatively

N. Navab and P. Jannin (Eds.): IPCAI 2010, LNCS 6135, pp. 135–146, 2010.

bounded time frame, once he has gained access to the valve, regarding the course of the valvuloplasty. A preoperative planning process elucidating which valvuloplasty option is most likely to result in a successful outcome (i.e., a *competent* valve) would therefore be highly useful to the cardiothoracic surgeon.

We describe our work with regard to segmentation, structure recovery and modeling, to address the goal of predicting the ability of a modified valve to be competent: the ability of the valve leaflets to coapt and thereby prevent any blood regurgitation from the left ventricle back into the left atrium, a condition potentially resulting in congestive heart failure. We initiate our process with an open 3D valve structure at end diastole, which was derived by segmenting 3D TEE data and was edited by a physician to remove artifacts and reflect the planned surgical modifications. From the open valve structure, we then infer the configuration of the valve leaflets at or near the end of isovolumic contraction to characterize coaptation.

Early heart modeling efforts can be traced back to the pioneering work by Peskin [3][4] in the '70s and '80s, that introduced the "immersed boundary" (IB) approach [5], which is still being refined and extended [6]. Yoganathan [1][7] reported Fluid Structure Interaction methods (FSI) extending IB to solve for the left-ventricle motion using 3D incompressible Navier-Stokes equations. [8] uses FSI for heart valve modeling. Watton [6] extended IB to simulate a polyurethane replacement valve placed in a cylindrical tube, subject to physiologic periodic fluid flow. Einstein [9] reported a coupled FSI mitral model immersed in a domain of Newtonian blood. This model had anterior and posterior leaflets but did not include other structures such as the left ventricle. Espino's 2D modeling work [10] simulated the left ventricle-generated blood flow by adding a non-anatomical inlet at the left ventricular apex. Other notable recent efforts and related projects include [13][14][15][16][17] and [18]. Most prior modeling work does not exploit patient specific anatomical data, with some recent exceptions that are focused on higher resolution medical imaging modalities such as MRI and CT [11][12]. Our approach differs from prior work, in that it incorporates patient-specific anatomical and dynamic information derived from 3D TEE. 3D echocardiography has several shortcomings when compared to MRI and

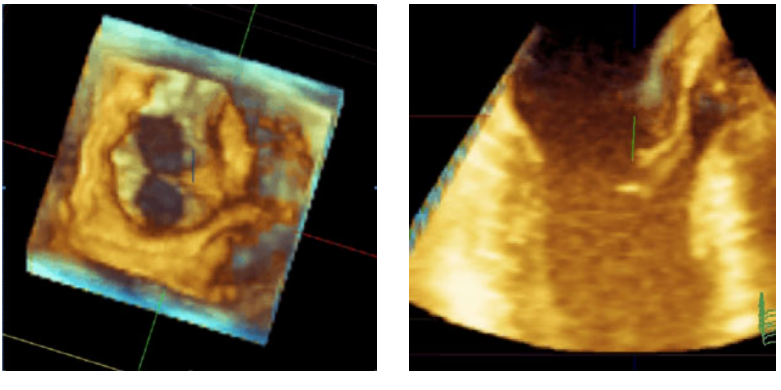

Fig. 1. A 3D TEE view of the mitral valve in the open position during diastole as seen from the atrium (left image) and a side view of the valve showing the anterior leaflet in front of the aortic valve (right image)

CT, including lower spatial resolution, and imaging artifacts including noise and obscuration. However, it has a number of advantages: it is non-ionizing, real-time, lower cost, it can be used pre- and intraoperatively, and allows interactive exploration.

Our valve mechanical modeling is also novel and takes its inspiration from methods characterizing cloth and sail behavior [21][22][23][24]. Sections 2 and 3 describe our approaches for structure recovery and modeling, while Sections 4 and 5 report experimental results and conclude.

2 Valve Segmentation

TEE segmentation is employed to recover the valve's static 3D structure that is then used in our mechanical modeling. We utilize an interactive user-in-the-loop approach that leverages two main automated methods to detect the valve leaflets and to find the boundaries of the heart's atrial and ventricular cavities.

A dynamic contour method is used to find the inner heart wall boundaries of the atrial and intraventricular cavities. This is complemented by a thin tissue detector that specifically finds the valve leaflets. The two methods are complementary, as the leaflets may not always be accurately segmented out by the dynamic contour approach, and the heart walls and valve annulus are generally not found by the thin tissue detector. The thin tissue detector models the local TEE intensity as Gaussian and then performs an analysis of the disparities of the eigenvalues associated with the intensity Hessian [25]. If one these eigenvalues is small when compared to the other two, this suggests the presence of a sheet or thin tissue structure. Another method we have used successfully to find thin tissues relies on morphological outlining.

The dynamic contour method used to find the heart inner walls exploits a level set approach and is summarized as follows: At time t=0, a dynamic contour is manually initialized in the atrial and/or intraventricular cavities. This dynamic contour is then obtained at any subsequent time t by considering an evolving function $\psi(x, y, z, t)$. The dynamic contour is found as $S(t)$, the zero level set of $\psi(.)$, i.e. $S(t) = \{(x, y, z) \mid \psi(x, y, z, t) = 0\}$. In our application, $\psi(.)$ evolves under a driving force which is designed to expand the contour until it reaches the intensity boundaries marking the inner walls of the atrial and ventricular cavities. An inhibition function $g(.)$, detailed later, stops the dynamic curve when it meets these walls boundaries.

Our specification of the evolution equation of $\psi(.)$ is inspired by the recent variational approach introduced by Li [19] that includes a penalty term $P(\psi)$ to evolve ψ so that, at all times, it closely approximates a signed distance function, a desirable feature for the determination of the zero level set $S(t)$. This penalty is expressed as

$$P(\psi) = \int_{\Omega} \frac{1}{2}\left(|\nabla \psi| - 1\right)^2 dx dy dz \tag{1}$$

where $\Omega \subset \mathbb{R}^3$ is the domain of ψ. The time evolution equation is then expressed as

$$\frac{\partial \psi}{\partial t} = -\frac{\delta \varepsilon}{\delta \psi} \tag{2}$$

where the r.h.s. denotes the Gâteaux derivative. The energy $\varepsilon(\psi)$ is defined as

$$\varepsilon(\psi) = \mu P(\psi) + \varepsilon_m(\psi) \tag{3}$$

and includes a model energy term $\varepsilon_m(\psi)$ that drives the contour's evolution to the desired goals, with a balancing weight $\mu > 0$. The primary goal of $\varepsilon_m(\psi)$ is to expand or contract the contour by expanding or contracting its enclosed volume $V_g(\psi)$, while keeping this contour simple, which is done by constraining the boundary area $A_g(\psi)$. The term $\varepsilon_m(\psi)$ is therefore specified as

$$\varepsilon_m(\psi) = \lambda A_g(\psi) + \nu V_g(\psi) \tag{4}$$

where λ and ν are weights balancing the boundary area and volume terms. These terms are respectively expressed as

$$A_g(\psi) = \int_\Omega g\delta(\psi)|\nabla \psi| \, dxdydz \tag{5}$$

$$V_g(\psi) = \int_\Omega gH(-\psi) \, dxdydz \tag{6}$$

where $\delta(\psi)$ denotes the Dirac delta function, and $H(\psi)$ is the Heaviside function. The weight ν is chosen here to be negative so that the contour expands. We note that these terms contain the inhibition function $g(\cdot)$ mentioned earlier, that is designed to abate the motion of the dynamic boundary in places corresponding to the heart wall location. This location can be indicated by a change in intensity and the presence of an edge in the 3D TEE. If considering the presence of an edge, the function g can be designed as

$$g(x, y, z) = \frac{1}{1 + a\,|\nabla G * I(x, y, z)|^2} \tag{7}$$

where $\nabla G * I$ is the gradient of the Gaussian-smoothed TEE intensity. This function represents a 'negative' of the gradient magnitude map, taking small values for high gradient magnitudes, and values close to 1 for small gradient magnitudes.

This gradient-based definition of $g(.)$ might be unsuitable for echocardiography images with limited contrast. However, we have found that transesophageal echocardiography imaging, which allows a direct 'view' into the left heart complex and specifically the mitral valve, often exhibits good contrast when compared to other ultrasound imaging or heart echocardiography approaches such as transthoracic echocardiography. Alternatively, a term emphasizing image intensity can be used for echocardiographic imagery with lesser contrast. In this case the inhibition function

$g(.)$ is designed to measure the departure in intensity from the intensity of the heart wall cavity, expressed as

$$g(x,y,z) = 1 - \frac{M(I(x,y,z),m,\sigma)}{M_{\max}} \tag{8}$$

where $M(I(x,y,z),m,\sigma) = \left(I(x,y,z)-m\right)^2 / \sigma^2$, $M_{\max} = \max(M(.))$ over the entire TEE cube, and (m,σ^2) are the mean and variance computed over the initial inner patch specified by the dynamic contour at time zero within the heart inner cavity.

In sum, regrouping all terms together in Eq. (2), and using the Gâteaux derivative it can be shown that the evolution of ψ is finally expressed as

$$\frac{\partial \psi}{\partial t} = \mu\left[\Delta\psi - \mathrm{div}\left(\frac{\nabla\psi}{|\nabla\psi|}\right)\right] + \lambda\delta(\psi)\,\mathrm{div}\left(g\frac{\nabla\psi}{|\nabla\psi|}\right) + \nu g\delta(\psi) \tag{9}$$

where div denotes the divergence and Δ the Laplacian operators. This equation specifies a time-update evolution equation $\partial\psi/\partial t$ which corresponds to a form of steepest descent. This equation is discretized to evolve the function ψ so as to minimize the objective functional $\varepsilon(\psi)$.

3 Computation of the Closed Valve Configuration

In contrast to other work concerned with computation of the valve dynamics or the left heart hemodynamics [2], this paper reports on work aiming to design a mechanical model of the valve specifically developed to infer the closed position of the valve (at or near the end of isovolumic contraction during systole) from open position (at end diastole) or vice versa. This is of particular interest in cases where one desires to answer the following question: given a hypothetical, patient specific, valve geometry modified to reflect the planned valvuloplasty, or given a surmised configuration of the chordae tendinae, or given the placement of a ring, does the novel valve geometry have the potential to come to a closed position where the leaflets may coapt? As argued earlier, this capability is useful for surgical planning. This capability is also of interest for diagnostics or as a way of generating additional data for image simulation and rendering for education and training purposes.

The method we use for stationary modeling of the closed valve is inspired by shape-finding finite element approaches applied to fabric ([21] through [24]). We have chosen this approach because the valve leaflets are very thin structures made up of connective tissue with elastic properties (tensile, compressive and bending modulus) similar to some types of thin cloth and fabric. A related method was recently applied to model the shape of spinnaker sails for the Swiss team that won the 2007 America's Cup.

The valve modeling is performed as follows. A mesh is defined on the leaflets based on the segmentation results. At each node of the mesh we prescribe either displacements or forces. Forces modeled include those due to fluid pressure, gravity, linear elastic stress, collision with other portions of the mesh, and tethering of the valve to the chordae tendinae themselves attached to papillary muscles.

The specified initial configuration of the open mesh is used to specify the zero energy point for external (fluid, gravity, etc.), elastic, and tethering forces. The zero energy point for the collision force is the configuration in which all facets of the mesh are not contacting (more specifically, further apart than a distance δ). Our goal is to find the configuration of the valve system at closed position where all forces are at equilibrium. This steady state is found by solving an energy minimization problem where we seek a stationary point that corresponds to a minimum for the energy.

For any given displacement of the nodes from the initial open configuration, and for each node *i*, we define the total energy ϕ of the displaced system as

$$\phi = \sum_i \phi_i \tag{10}$$

along with the forces $\mathbf{F}_i = -\nabla\phi_i$. We consider the following additive components for the energy

$$\phi_i = \phi_i^X + \phi_i^E + \phi_i^T + \phi_i^C + \phi_i^K \tag{11}$$

including: ϕ_i^X , the external energy, ϕ_i^E , the elastic energy, ϕ_i^T , the tethering energy, ϕ_i^C the collision energy, and ϕ_i^K , the kinetic energy. The kinetic energy is neglected here since we are interested in directly solving for the system state in closed position where the velocity is negligible. The other significant energy terms are specified next.

External energy

The external energy results from external forces exerted on the leaflets such as the intraventricular blood pressure forces and gravity. This energy is assumed to be due to a set of fields of constant force $\{\mathbf{f}^k\}$ such that

$$\phi_i^X = -\sum_k \mathbf{f}^k \bullet \mathbf{d}_i \tag{12}$$

where $\mathbf{d}_i$ is the displacement of node *i*, and the index *k* ranges over the external force fields to which the leaflets are subject, including gravity and blood intraventricular force field. Gravity is not considered here since this term is negligible when compared to the energy due to intraventricular pressure. Our external force direction is specified so as to be oriented toward a 3D line that goes through the two commissure points of the valve (the points at which the two leaflets join).

Elastic energy

The elastic energy is given by

$$\phi_i^E = \sum_{\substack{\text{facets } j \\ \text{containing} \\ \text{node } i}} \frac{1}{2}\boldsymbol{\sigma}_j \bullet \boldsymbol{\varepsilon}_j \tag{13}$$

where $\boldsymbol{\varepsilon}_j = \left(\varepsilon_{xx}, \varepsilon_{yy}, \varepsilon_{xy}\right)^T$ is the strain vector determined from the fractional displacements of the nodes of the facet j [24] and $\boldsymbol{\sigma}_j = \left(\sigma_{xx}, \sigma_{yy}, \sigma_{xy}\right)^T = \mathbf{H}\boldsymbol{\varepsilon}_j$ is the stress vector of the facet j. Here,

$$\mathbf{H} = \frac{E}{1-\nu^2}\begin{pmatrix} 1 & \nu & 0 \\ \nu & 1 & 0 \\ 0 & 0 & 1-\nu \end{pmatrix} \tag{14}$$

is the elasticity matrix of the mesh, written in terms of Young's modulus of elasticity, E, and Poisson's ratio, ν. Note that while, in general, a hyperelastic assumption is used and may more accurately model certain biological tissue properties, we feel that this is unnecessary in the case of the valve modeling due to the leaflets' specific nature, i.e., very thin and flexible but highly inelastic. The small amount of leaflet stretching can be accurately modeled using a linear stress-strain relationship, while the primary mode of deformation is deflection of the leaflet. We assume that energy associated with folding along the edges of the finite elements is small compared to energy due to external forces and hence elastic resistance to leaflet deflection can be neglected.

Tethering energy

The tethering energy is used to include the effects of the chordae tendinae whose function is to restrict the range of motion of the leaflets thereby preventing prolapse in healthy valves. Since these chords are quasi-inextensible, this energy is specified as

$$\phi_i^T = \begin{cases} \Phi^t \dfrac{\left(\left|\mathbf{p}_i - \mathbf{q}_i\right| - r_i\right)^3}{\rho^3} & if\ \left|\mathbf{p}_i - \mathbf{q}_i\right| > r_i \\ 0 & otherwise \end{cases} \tag{15}$$

Where Φ^t is the strength of the tethering force, $\mathbf{p}_i$ is the position of the displaced node i, $\mathbf{q}_i$ is the position of the point to which node i is tethered, r_i is the chord length, and ρ is the scale of the range dependence of the force. Some of the nodes located at the leaflets' rims are selected and subject to tethering forces to simulate attachment to the primary mitral chordae tendinae. Secondary and tertiary chordae effects can be neglected for this application although their configuration does impact the overall systolic pressure distribution and they should be considered for dynamic simulation.

Collision energy

The collision energy ϕ_i^C is given by considering a repulsive force between all nodes

$$\phi_i^C = \sum_{\substack{facets\ T_j \\ containing \\ node\ i}} \sum_{\substack{facets\ T_k \\ not\ adjacent \\ to\ facet\ T_j}} \int_{T_j} d\mathbf{r}_j \int_{T_k} d\mathbf{r}_k e\left(\left|\mathbf{r}_j - \mathbf{r}_k\right|\right) \tag{16}$$

where the facet point $\mathbf{r}_j$ (resp. $\mathbf{r}_k$) spans the region of the facet T_j (resp. T_k) and $e(d)$ specifies a repulsive energy dependent on the distance d between the interacting facet points and is defined as

$$e(d) = \begin{cases} \Phi^C \left(1 - \frac{d}{\delta}\right)^n & \text{if } d < \delta \\ 0 & \text{otherwise} \end{cases} \tag{17}$$

where Φ^C specifies the strength of the repulsive force. Defining the collision energy in such a fashion allows us to address self collision effects. The double summation is only considered between facets which are 'close' to each other, and we use an efficient tree-based range search to restrict the computational impact of this summation. This is an important consideration since the computation of the collision energy is a major factor contributing to total computational load. The range δ specifies the interacting node distance under which the collision force becomes active. Since the double integral term is evaluated by further discretizing points within the facet, this range should be set to a value that is of the order of the smallest distance between the mesh nodes. Therefore, at the final configuration, the remaining gap between colliding/coapting leaflets will be of the order of the mesh facet resolution. The mesh resolution can be tuned down to generate smaller gaps thereby trading slower convergence for finer precision. Since a planning tool is meant to allow the clinician to test various candidate solutions, a moderate mesh resolution that would still allow to answer the question of whether the leaflets have potential to coapt and the valve to be competent, should be sufficient.

The variation of total potential energy is a function of 3N displacement coordinates where N is the number of free nodes. We define a plane including the valve annulus and all 'top' nodes on the other side of this plane are kept static during the optimization process. To find the closed position of the leaflets given the distributed forces and imposed displacements, we find the configuration which minimizes the total energy by using the BFGS (Broyden Fletcher Goldfarb Shanno) quasi-Newton optimization process implemented in the Matlab Optimization Toolbox. Additional constraints may be used to augment this model: one such possibility is to add a constraint to model the addition of a ring around the valve annulus to simulate the surgical insertion of a ring to render the valve more competent.

4 Experiments

Intra-operative real-time 3D TEE full volume data of mitral valves were obtained from several patients using an iE33 Philips console fitted with a Philips X2-T Live 3D TEE probe (Philips Medical Systems, Bothell, WA). The data was semi-automatically segmented using the method described in Section 2. Examples of segmentation of 2D TEE planes and full 3D TEE cubes are shown in Figure 2. The automated segmentation was followed by visual inspection and user-in-the-loop correction to edit out artifacts due to ultrasonic imaging, and to complete some anatomical structures missing because of obscuration or limitations of the TEE field of view.

User intervention is also used to modify the valve in a way that reflects a plausible surgical valvuloplasty. Figure 2 shows segmentation results obtained using the level set inner heart cavities segmentation, and the thin tissue leaflet detection, prior to user intervention. The thin tissue methods give satisfactory results and, as expected, tend to omit sections of the annulus that can be reconstructed through the level set method. The level set method tends to do better with the intraventricular and atrial walls, which can then be combined with the thin tissue method for a complete segmentation. We found results to be generally acceptable although some challenges still remain: it is often difficult to completely discern where the valve ends and the chordae start. However this is to be expected since the chords' anatomy consists of an intricate extension of the valves' extremities, and both structures are made up of similar types of tissue that are rich in collagen and elastin fibers. The segmented valve was converted to a mesh and, as a final processing step, a nearest neighbor mesh smoothing filter was applied.

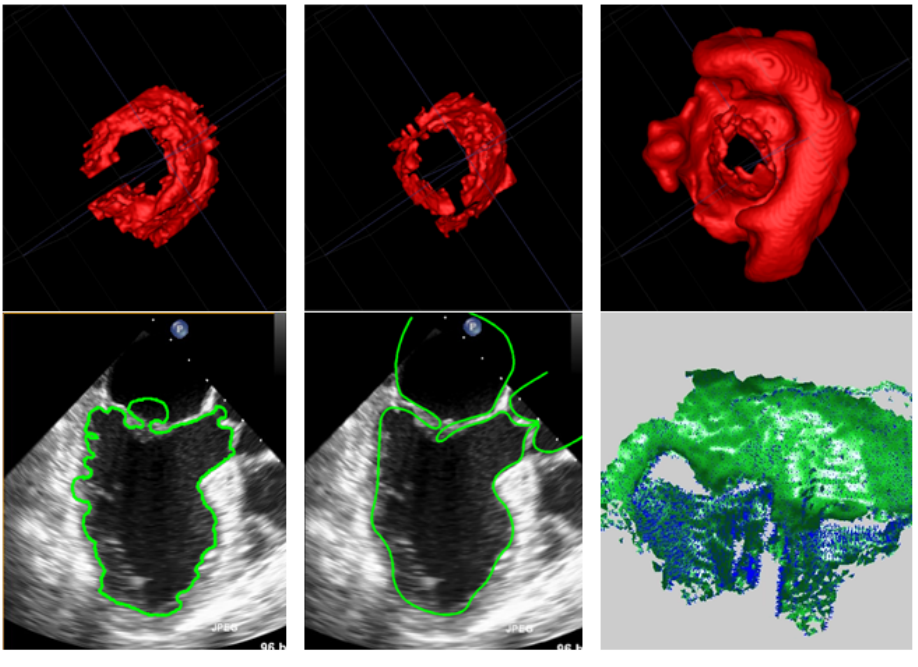

Fig. 2. 2D Examples of segmentation of the mitral valve and heart walls: using a morphology-based thin tissue detection (top left); using a Hessian-based thin tissue detection (top middle); using level sets (top right). 2D segmentation of a 3D TEE planar slice before and after user modifications (bottom left and middle); final 3D segmentation including valve and internal heart wall cavities with surface normals shown, after user modifications (bottom right).

The segmented 3D mesh obtained at a frame corresponding to the open valve position was used to model and predict the configuration at end systole (Figures 3 and above). Figure 3 shows the initial and final computed configurations. The color coded surfaces show in blue and orange the facets corresponding to the anterior and posterior

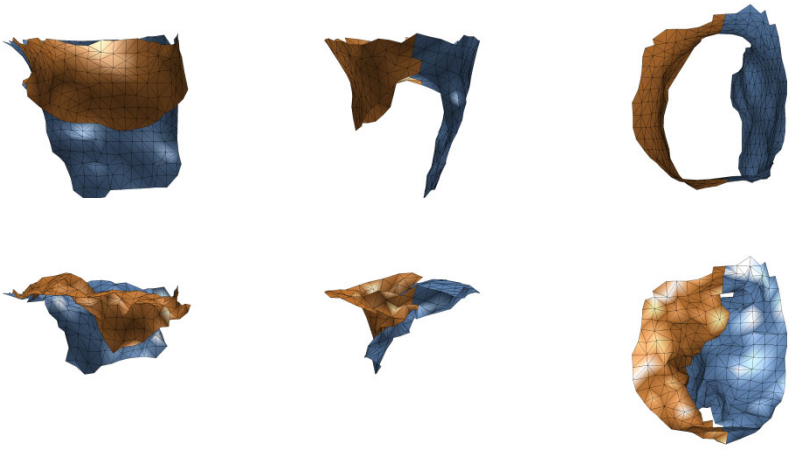

Fig. 3. Initial open valve configuration from TEE segmentation (top) and closed configuration computed by mechanical modeling at near end systole (bottom)

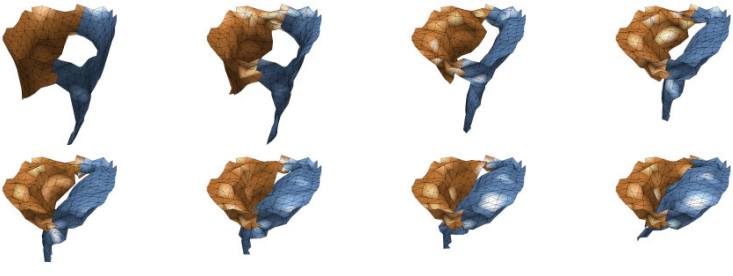

Fig. 4. Sequence of computed configurations taken at various intermediary iterations

leaflets. As is seen from the various views, the collision computation worked correctly as there is no surface crossing. In this example, the valve geometry was deemed to be capable of coapting everywhere except in an area close to the commissure points where the leaflets are too short to contact. This illustrates the potential difficulty during segmentation in discerning where the valve ends and the chordae tendinae begin, which in turn may lead to the segmented leaflets to be shorter than they actually are. A sequence of intermediary configurations in Figure 4 shows that although this model was developed to solve a stationary problem, the intermediary states give a plausible kinematic description of the leaflets' motion. This is because the kinetic energy of the valve leaflets is probably negligible when compared to the other energy terms during closure, in particular the external energy due to intraventricular pressure.

We performed experiments using several 3D TEE sequences taken from patients at JHU SOM. Validation was carried out by manual registration and comparison of (a) the closed valve configuration predicted at end systole from the segmented open valve captured at end diastole, with (b) the actual closed valve structure segmented at end systole (see Figure 5) and found an average difference of 4 to 5 mm. This is a

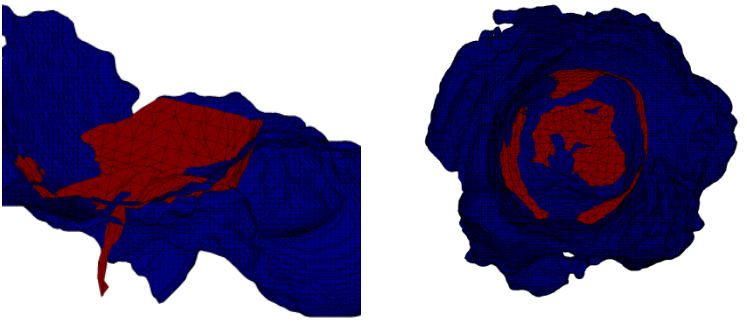

Fig. 5. Comparison of computed closed configuration (red) overlaid and registered with closed configuration segmented from 3D TEE (blue) acquired at end systole (side and top views). Close inspection reveals a good fit between the computed and actual configurations. We also inferred differences which are of the order of the errors made by the segmentation step, indicating good performance for the modeling step.

promising result considering that the TEE resolution is of the order of 1 mm and segmentation has an average error of about 1 to 2 mm depending on the method used.

5 Conclusions

We proposed a novel patient-specific mitral valve surgical planning method to help characterize the competency of a virtually modified valve. The novelty of our approach is twofold: (a) we exploit prior structural information derived from segmentation of 3D TEE, and (b) we propose a novel valve leaflet modeling approach based on the modeling of cloth. Preliminary results are presented and show the promise of the approach. Future goals are to address certain limitations of the segmentation and modeling methods, augment the model by incorporating physiological blood pressure forces, and carry out further clinical validation.

References

[1] Sacks, M.S., Yoganathan, A.P.: Heart valve function: a biomechanical perspective. Philos. Trans. R. Soc. Lond. B. Biol. Sci. 362, 1369–1391 (2007)

[2] Sprouse, C., Yuh, D., Abraham, T., Burlina, P.: Computational Hemodynamic Modeling based on Transesophageal Echocardiographic Imaging. In: Proc. IEEE Engineering in Medicine and Biology Conference, Minneapolis (September 2009)

[3] Peskin, C.S.: Flow patterns around heart valves. a digital computer method for solving the equations of motion. Albert Einstein College of Medicine, Ph.D (1972)

[4] Peskin, C.S.: Mathematical aspects of heart physiology: Courant Institute of Mathematical Sciences (1975)

[5] Peskin, C.S., McQueen, D.M.: A 3D computational method of blood flow in the heart: 1. immersed elastic fibers in a viscous incompressible fluid. Journal Computational Physics 81, 372–405 (1989)

[6] Watton, P.N., Luo, X.Y., Singleton, R., Wang, X., Bernacca, G.M., Molloy, P., Wheatley, D.J.: Dynamic modeling of prostetic chorded mitral valves using the immersed boundary method. In: IEEE Conf. Engineering in Medicine and Biology Society (2004)
[7] Vesier, C.C., Lemmon, J.J.D., Levine, R.A., Yoganathan, A.P.: A three-dimensional computational model of a thin-walled left ventricle. In: Proceedings of the 1992 ACM/IEEE conference on Supercomputing (1992)
[8] Loon, R.v., Anderson, P.D., van de Vosse, F.N.: A fluid-structure interaction method with solid-rigid contact for heart valve dynamics. Jounal of Computational Physics 217, 806–823 (2006)
[9] Einstein, D., Kunzelman, K., Reinhall, P., Nicosia, M., Cochran, R.: Non-linear fluid-coupled computational model of the mitral valve. J. Heart Valve Dis. 14, 376–385 (2005)
[10] Espino, D., Watkins, M.A., Shepherd, D.E.T., Hukins, D.W.L., Buchan, K.G.: Simulation of blood flow through the Mitral Valve of the heart: a fluid structure interaction model. In: Proc. COMSOL Users Conference (2006)
[11] Hu, Z., Metaxas, D., Axel, L.: Computational modeling and simulation of heart ventricular mechanics with tagged MRI. In: ACM symposium on Solid and physical modeling 2005 (2005)
[12] Hammer, P., Nido, P.d., Howe, R.: Image based mass spring model of mitral valve closure for surgical planning. In: SPIE Medical (2008)
[13] Bassingthwaighte, J.B.: Design and strategy for the Cardionome project. Adv. Exp. Med. Biology (1997)
[14] Delinghette, H.: Integrated cardiac modeling and visualization. In: Int. Conf. Medical Image Computing and Computer-Assisted Intervention (2008)
[15] INRIA-REO, The INRIA REO group (2008)
[16] Santos, N.D.D., Gerbeau, J.-F., Bourgat, J.F.: A partitioned fluid-structure algorithm for elastic thin valves with contact. Comp. Meth. Appl. Mech. Eng. 197 (2008)
[17] Astorino, M., Gerbeau, J.-F., Pantz, O., Traoré, K.-F.: Fluid-structure interaction and multi-body contact. Application to the aortic valves, INRIA RR 6583 (2008)
[18] EU, The virtual physiological human EU project (2008)
[19] Li, C., Xu, C., Gui, C., Fox, M.: Level Set Evolution without Re-Initialization: A New Variational Formulation, pp. 430–436 (2005)
[20] Corsi, C., Saracino, G., Sarti, A., Lamberti, C.: Left ventricular volume estimation for real-time three-dimensional echocardiography. IEEE Trans. Medical Imaging 21 (2002)
[21] Maître, O.L., Huberson, S., Souza de Cursi, E.: Unsteady Model of Sail and Flow Interaction. Journal of Fluids and Structures 13, 37–59 (1998)
[22] Charvet, T., Huberson, S.G.: Numerical Calculation of the flow around sails. European Journal of Mechanics 11, 599–610 (1992)
[23] Hauville, F., Mounoury, S., Roux, Y., Astolfi, J.E.: Equilibre dynamique d'une structure idealement flexible dans un ecoulement: application a la deformation des voiles. Journees AUM AFM. Brest (2004)
[24] Arcaro, V.F.: A Simple Procedure for Shape Finding and Analysis of Fabric Structures, `http://www.arcaro.org/`tension
[25] Huang, A., Nielson, G., Razdan, A., Farin, G., Baluch, D., Capco, D.: Thin structure segmentation and visualization in three-dimensional biomedical images: a shape-based approach. IEEE Transactions on Visualization and Computer Graphics 12, 93–102 (2006)